Gastroenterology 2023;164:1310–1313

RESEARCH LETTERS

RNA Sequencing Identifies Frequent Mitogen-activated Protein Kinase–associated Fusion Genes in Intraductal Tubulopapillary Neoplasms of the Pancreas

Intraductal tubulopapillary neoplasms (ITPNs) of the pancreas are rare cystic precursor neoplasms to invasive pancreatic ductal adenocarcinoma (PDAC) and account for 3% of intraductal neoplasms of the pancreas. Originally reported by Yamaguchi et al,[1] the clinicopathologic features of ITPNs are distinct from other pancreatic cysts. Radiographically, ITPNs are characterized by a nodular mass within dilated pancreatic ducts (Supplementary Figure 1*A* and *B*). These nodules are histologically composed of a tubulopapillary growth of epithelium with scant cytoplasmic mucin and necrotic foci (Supplementary Figure 1*C–E*).[2] In addition to their architectural complexity, ITPNs uniformly exhibit high-grade cytologic atypia and, in most cases, have an associated invasive carcinoma component (Supplementary Figure 1*F–H*).

Although the morphologic features of ITPNs are clearly defined, the pathogenesis of these neoplasms remains poorly understood. The genomic findings of ITPNs differ significantly from those that are typically seen in other cystic precursor neoplasms of the pancreas and PDAC. Mutations in *KRAS* and *GNAS* are often absent in ITPNs, whereas these genomic alterations are frequently detected in intraductal papillary mucinous neoplasms and associated PDAC. Other than a subgroup of ITPNs harboring *FGFR2* fusion genes and mutations within chromatin remodeling genes (eg, *BAP1*) and genes associated with the mechanistic target of rapamycin signaling pathway (eg, *PIK3CA*), recurrent driver genes have yet to be described in ITPNs.[3,4] In fact, some ITPNs do not harbor alterations in genes associated with PDAC. Considering *KRAS* wild-type PDACs often harbor alternative drivers of the mitogen-activated protein kinase (MAPK) signaling pathway, we performed both DNA- and RNA-based targeted next-generation sequencing (NGS) and whole transcriptome sequencing (WTS) of 23 surgically resected ITPNs (Supplementary Material and Methods).

Consistent with previous studies, targeted NGS detected *KRAS* missense mutations in a minority of ITPNs (n = 2, 9%) (Table 1). However, alterations in genes coding for members of the MAPK signaling pathway were also identified and included a *BRAF* missense mutation (n = 1), *ERBB2* amplification (n = 1), *STRN-ALK* fusion gene (n = 1), *BRAF* fusion genes (*SND1-BRAF* and *AGK-BRAF*, n = 2), *ATP1B1-NRG1* fusion gene (n = 2), *TRIM24-RET* (n = 1), and multiple *FGFR2* fusion genes (*FGFR2-BICC1*, *FGFR2-CIT*, *FGFR2-FAM76A*, *FGFR2-PPHLN1*, and *FGFR2-NOL4*; n = 5). Fifteen of 23 ITPNs (65%) had MAPK driver alterations and 11 ITPNs (48%) harbored fusion genes, which were mutually exclusive from each other. Additional alterations in decreasing order occurred in *TP53* (n = 10), *SMAD4* (n = 9), *CDKN2A* (n = 7), chromatin remodeling genes (*BAP1* and *ARID1A*, n = 5), homologous recombination-related genes (*BRCA2* and *CHEK2*, n = 3), *STK11* (n = 2), Myc family of oncogenes (*MYC* and *NMYC*, n = 2), and *PTEN* (n = 1). Moreover, multiple chromosomal abnormalities were identified in 10 ITPNs (43%).

Considering the relative abundance of MAPK-associated fusion genes that were found by targeted NGS, we hypothesized that additional fusion genes may be present among the 8 ITPNs (35%) without a discernable MAPK driver alteration. Therefore, we performed WTS and detected fusion genes in the remaining 8 ITPNs: *FGFR2-TACC2* (n = 2), *CFTR-RASGRF2* (n = 1), *SPTLC1-JAK2* (n = 1), *ATXN3-MAML3* (n = 1), *NCOA3-MAML2* (n = 1), *RUNX2-MAML2* (n = 1), and *ATXN3-MAML2* (n = 1) (Supplementary Figure 2). Analogous to the results of targeted NGS, each fusion gene was mutually exclusive from other fusion genes, thus suggesting their involvement in common pathologic mechanisms. Because many of these fusion genes have not been described in other neoplasms, fluorescence in situ hybridization using *MAML2* break-apart probes (orange, 5′ end of *MAML2*; green, 3′ end of *MAML2*) was performed on cases 21, 22, and 23 and confirmed the presence of a *MAML2* rearrangement (Supplementary Figure 3). Additionally, the ITPN-associated PDAC for cases 8, 10, 11, and 16 were evaluated by either targeted NGS or WTS, and the respective fusion identified within the ITPN was also detected. Matched preoperative pancreatic cyst fluid specimens were available for a subset of ITPNs (cases 6, 8, 10, and 13), and once again the respective fusion genes were identified.

Overall, 17 of 23 ITPNs (74%) were found to have MAPK driver alterations that included fusion genes and were mutually exclusive from each other. These fusion genes were also present within corresponding ITPN-associated PDACs and detected in preoperative pancreatic cyst fluid. Among the remaining 6 ITPNs, novel fusion genes were identified that were once again mutually exclusive from other fusion genes and included the following: *CFTR-RASGRF2*, *SPTLC1-JAK2*, *ATXN3-MAML3*, *NCOA2-MAML2*, *RUNX2-MAML2*, and *ATXN3-MAML2*. Fusion genes involving *RASGRF2* and *JAK2,* but with different 5′ partners, have been previously reported in melanocytic lesions and hematologic

Abbreviations used in this paper: ITPN, intraductal tubulopapillary neoplasm; MAPK, mitogen-activated protein kinase; MEC, mucoepidermoid carcinoma; NGS, next-generation sequencing; PDAC, pancreatic ductal adenocarcinoma; WTS, whole transcriptome sequencing.

Most current article

0016-5085
https://doi.org/10.1053/j.gastro.2023.02.006

Table 1. Clinicopathologic Findings of 23 Patients With an ITPN of the Pancreas

Case no.	Age (y)	Sex	Location	Size (cm)	Associated carcinoma	Gene fusion	Other genomic alterations
1	64	M	Pancreatic head	1.1	Yes	None	*KRAS* p.G12V, *TP53* p.R248W, *TP53* deletion, *CDKN2A/B* deletion, *STK11* deletion, *MYCN* amplification (25 copies)
2	75	M	Pancreatic body and tail	7.0	Yes	None	*KRAS* p.G12R, *TP53* p.L194R, *TP53* deletion, *CDKN2A/B* deletion, *SMAD4* deletion, chromosomal gain of 11q, chromosomal loss of 16p
3	64	F	Pancreatic body	2.7	Yes	None	*BRAF* p.V600E, chromosomal gain of 1q, chromosomal loss of 1p
4	69	F	Pancreatic body and tail	9.0	Yes	None	*ERBB2* amplification (19 copies), *TP53* p.T125_splice, *ARID1A* p.A245Gfs*113
5	34	M	Pancreatic head	7.5	Yes	*STRN-ALK*	*TP53* deletion, *SMAD4* deletion
6[a]	62	M	Pancreatic head	3.8	No	*SND1-BRAF*[b]	*TP53* deletion
7	18	F	Entire pancreas	18.0	No	*AGK-BRAF*	*TP53* deletion, *SMAD4* deletion, chromosomal gain of 7p and 7q, chromosomal loss of 6p and 6q
8[a]	59	M	Pancreatic body and tail	3.5	Yes[c]	*ATP1B1-NRG1*[b]	*SMAD4* deletion
9	79	M	Entire pancreas	26.6	Yes	*ATP1B1-NRG1*	*SMAD4* deletion, *CHEK2* p.S372F, chromosomal loss of 1p, 6q, and 16p
10[a]	68	F	Pancreatic body and tail	6.4	Yes[c]	*TRIM24-RET*[b]	*CDKN2A/B* deletion, *SMAD4* deletion, chromosomal gain of 1q and 12q, chromosomal loss of 1p and 14q
11	61	F	Pancreatic head	5.0	Yes[c]	*FGFR2-BICC1*	*CDKN2A/B* deletion
12	27	F	Pancreatic head	3.5	Yes	*FGFR2-CIT*	*BAP1* p.F46Lfs*26, *CDKN2A/B* deletion
13[a]	81	F	Pancreatic body	3.9	No	*FGFR2-TACC2*[b]	*TP53* p.R273H, *MYC* amplification (16 copies)
14	73	M	Pancreatic head	8.0	Yes	*FGFR2-FAM76A*	*TSC1* p.E1101*
15	63	M	Pancreatic body and tail	7.5	Yes	*FGFR2-PPHLN1*	*BAP1* splice site c.376-33_378del36, *MYC* amplification (8 copies)
16	78	F	Pancreatic tail	5.4	Yes[c]	*FGFR2-TACC2*	*SMAD4* deletion, *ARID1A* p.Q581*, *ARID1A* deletion, chromosomal loss of 9p, 9q, 12q, and 14q
17	22	M	Entire pancreas	13.4	Yes	*FGFR2-NOL4*	*BAP1* splice site c.428-2A>G, *CDKN2A/B* deletion, *BRCA2* deletion
18	53	F	Entire pancreas	12.5	No	*CFTR-RASGRF2*	*MYC* amplification (7 copies), chromosomal gain of 1p
19	37	F	Pancreatic head	4.8	Yes	*SPTLC1-JAK2*	*SMAD4* deletion, *STK11* p.G196Afs*91
20	74	M	Entire pancreas	10.5	Yes	*ATXN3-MAML3*	*TP53* p.E346*, *TP53* deletion, *CDKN2A/B* deletion, *RB1* p.E580*, *RB1* deletion, *PTEN* p.D107Y, *PTEN* deletion
21	68	F	Pancreatic head	6.0	Yes	*NCOA3-MAML2*	*TP53* p.S241F, *TP53* deletion, *CDKN2A/B* deletion, *SMAD4* deletion, chromosomal loss of 11p, 11q, 13q, 19p, and 19q
22	73	F	Pancreatic head	3.1	Yes	*RUNX2-MAML2*	*TP53* deletion, *CDKN2A/B* deletion, *BRCA2* p.K2674*, *BRCA2* deletion, chromosomal loss of 17q
23	47	M	Pancreatic head	5.0	Yes	*ATXN3-MAML2*	*ARID1A* deletion, chromosomal loss of 11p and 11q

[a]In addition to the patient's surgical specimen, the corresponding preoperative specimen (pancreatic cyst fluid) was molecularly evaluated.
[b]The gene fusion was also detected within the patient's corresponding preoperative pancreatic cyst fluid.
[c]The gene fusion was also detected within the ITPN-associated invasive PDAC.

neoplasms, respectively, and shown to result in downstream MAPK activation.[5,6] Thus, although the *CFTR-RASGRF2* and *SPTLC1-JAK2* fusion genes have not been specifically described, these alterations likely represent genomic drivers of the MAPK signaling pathway. In further support that these fusion genes similarly affect the MAPK signaling pathway, WTS of 9 ITPNs (Supplementary Figure 4) identified analogous gene expression profiles among each ITPN; however, the profiles were distinctly different compared with 13 intraductal papillary mucinous neoplasms and further underscore that ITPNs are a separate neoplasm from intraductal papillary mucinous neoplasms.

The presence of *MAML2* and *MAML3* fusion genes in ITPNs is an intriguing finding. Both MAML2 and MAML3 belong to the 3-member transcriptional coactivator MAML (mastermind-like) family that plays an essential role in the transcriptional activation of multiple signaling pathways. However, our current understanding of the MAML proteins in cancer, such as mucoepidermoid carcinomas (MECs) of the salivary gland, is largely based on studies of the *CRTC1-MAML2* fusion gene. The generation of a genetically engineered mouse model has established CRTC1-MAML2 as a key oncoprotein in the pathogenesis of MECs.[7] Further, both in vitro cell line experiments and protein expression analysis of primary MECs have demonstrated that the *CRTC1-MAML2* fusion gene is associated with MAPK activation.[8] Blockade of the MAPK pathway with anti–epidermal growth factor receptor antibodies or pharmacologic inhibitors decreases cell growth and survival in *CRTC1-MAML2* fusion-positive MEC cell lines and human MEC xenografts. It is therefore reasonable to speculate that the ITPN-associated *MAML2* and *MAML3* fusion genes are oncogenic MAPK driver alterations.

There are limitations to our study. Although it represents one of the largest series of pancreatic ITPNs to be molecularly analyzed, the number of cases evaluated is relatively small, and concluding that driver alterations, especially fusion genes, within the MAPK signaling pathway are a universal feature of ITPNs may be premature. It is important to note, however, that ITPNs can arise from the bile duct and also represent precursor neoplasms to cholangiocarcinoma.[9] Sequencing studies of biliary ITPNs are limited, but mutations in *KRAS* and *BRAF* are of similar low prevalence in biliary ITPNs as pancreatic ITPNs.[10] Moreover, *FGFR2* alterations have been found in ITPNs of the bile duct. Considering the radiographic, histologic, and molecular parallels between pancreatic and biliary ITPNs, it is plausible that biliary ITPNs are also characterized by frequent MAPK-associated fusion genes. Unfortunately, WTS studies of biliary ITPNs have not been reported. Another issue with our study is the lack of orthogonal confirmation of all fusion genes described herein. Many fusion genes detected by targeted NGS were validated through WTS (Supplementary Material and Methods), and break-apart fluorescence in situ hybridization was used to confirm the presence of *MAML2* rearrangements. Additionally, the identification of the same fusion gene in matched preoperative pancreatic cyst fluid and corresponding ITPN-associated PDACs provides further support to the validity of our findings.

In summary, we report the results of targeted NGS and WTS of pancreatic ITPNs, and, consistent with previous findings, missense mutations in *KRAS* were seen in some cases. Notably, other genomic alterations implicated within the MAPK signaling pathway were identified in the remaining cases and were mutually exclusive from each other. The predominant genomic alteration found in ITPNs was the presence of a fusion gene, many of which have not been described in PDAC or other neoplasms. Finally, the detection of ITPN-associated fusion genes in preoperative pancreatic cyst fluid suggests these genomic alterations could potentially improve the early detection of these cystic precursor neoplasms to PDAC.

Supplementary Material

Note: To access the supplementary material accompanying this article, visit the online version of *Gastroenterology* at www.gastrojournal.org and at https://doi.org/10.1053/j.gastro.2023.02.006.

JAE W. LEE
Department of Pathology
Sol Goldman Pancreatic Cancer Research Center
Johns Hopkins University School of Medicine
Baltimore, Maryland

RALPH H. HRUBAN
Department of Pathology
Sol Goldman Pancreatic Cancer Research Center
Department of Oncology
Sidney Kimmel Comprehensive Cancer Center
Johns Hopkins University School of Medicine
Baltimore, Maryland

LODEWIJK A.A. BROSENS
Department of Pathology
University Medical Center Utrecht
Utrecht, The Netherlands

VINCENZO CONDELLO
MARINA N. NIKIFOROVA
AATUR D. SINGHI
Department of Pathology
University of Pittsburgh Medical Center
Pittsburgh, Pennsylvania

PANCREATIC CYST ALLIANCE

References

1. Yamaguchi H, et al. Am J Surg Pathol 2009;33:1164–1172.
2. Basturk O, et al. Am J Surg Pathol 2017;41:313–325.
3. Yamaguchi H, et al. Am J Surg Pathol 2011;35:1812–1817.
4. Basturk O, et al. Mod Pathol 2017;30:1760–1772.
5. Houlier A, et al. Pigment Cell Melanoma Res 2021;34:1074–1083.

6. Peeters P, et al. Blood 1997;90:2535–2540.
7. Chen Z, et al. JCI Insight 2021;6:e139497.
8. Chen Z, et al. Oncogene 2014;33:3869–3877.
9. Park HJ, et al. Pathol Int 2010;60:630–635.
10. Gross C, et al. Cancers 2021;13:2742.

Received May 13, 2022. Accepted February 7, 2023.

Correspondence
Address correspondence to: Aatur D. Singhi, MD, PhD, UPMC Presbyterian Hospital, 200 Lothrop Street, Room A616.2, Pittsburgh, Pennsylvania 15213. e-mail: singhiad@upmc.edu.

Acknowledgments
Members of the Pancreatic Cyst Alliance are as follows: James Tucker, PhD,[1] Amer H. Zureikat, MD,[2] Jin He, MD, PhD,[3] Alessandro Paniccia, MD,[2] Kenneth K. Lee, MD,[2] Herbert J. Zeh, MD,[4] Melissa E. Hogg, MD,[5] Anil K. Dasyam, MD,[6] Kevin McGrath, MD,[7] Anne Marie Lennon, MD, PhD,[8] Kenneth E. Fasanella, MD,[7] Elham Afghani, MD, MPH,[8] Randall E. Brand, MD,[7] Adam Slivka, MD, PhD,[7] Nisa Kubiliun, MD,[9] Christopher J. VandenBussche, MD, PhD,[10] Elizabeth D. Thompson, MD, PhD,[10] Michael S. Torbenson, MD,[11] Daniela S. Allende, MD,[12] Phoenix D. Bell, MD,[4] Cihan Kaya, PhD,[1] and Abigail I. Wald, PhD[1]; from the [1]Department of Pathology, University of Pittsburgh Medical Center, Pittsburgh, Pennsylvania; [2]Department of Surgery, University of Pittsburgh Medical Center, Pittsburgh, Pennsylvania; [3]Department of Surgery, Johns Hopkins University School of Medicine, Baltimore, Maryland; [4]Department of Surgery, University of Texas Southwestern, Dallas, Texas; [5]Department of Surgery, NorthShore University Health System, Evanston, Illinois; [6]Department of Radiology, University of Pittsburgh Medical Center, Pittsburgh, Pennsylvania; [7]Department of Medicine, University of Pittsburgh Medical Center, Pittsburgh, Pennsylvania; [8]Department of Medicine, Johns Hopkins University School of Medicine, Baltimore, Maryland; [9]Department of Medicine, University of Texas Southwestern, Dallas, Texas; [10]Department of Pathology, Sol Goldman Pancreatic Cancer Research Center, Johns Hopkins University School of Medicine, Baltimore, Maryland; [11]Department of Laboratory Medicine and Pathology, Mayo Clinic Rochester, Rochester, Minnesota; and [12]Department of Anatomic Pathology, Cleveland Clinic, Cleveland, Ohio.

CRediT Authorship Contributions
Ralph H. Hruban, MD (Conceptualization: Equal; Data curation: Equal; Formal analysis: Equal; Writing – original draft: Equal; Writing – review & editing: Equal).
Lodewijk A. A. Brosens, MD, PhD (Data curation: Supporting).
Vincenzo Condello, PhD (Data curation: Supporting).
James Tucker, PhD (Data curation: Supporting).
Amer H. Zureikat, MD (Data curation: Supporting).
Jin He, MD, PhD (Data curation: Supporting).
Alessandro Paniccia, MD (Data curation: Supporting).
Kenneth K. Lee, MD (Data curation: Supporting).
Herbert J. Zeh, MD (Data curation: Supporting).
Melissa E. Hogg, MD (Data curation: Supporting).
Anil K. Dasyam, MD (Data curation: Supporting).
Kevin McGrath, MD (Data curation: Supporting).
Anne Marie Lennon, MD, PhD (Data curation: Supporting).
Kenneth E. Fasanella, MD (Data curation: Supporting).
Elham Afghani, MD, MPH (Data curation: Supporting).
Randall E. Brand, MD (Data curation: Supporting).
Adam Slivka, MD, PhD (Data curation: Supporting).
Nisa Kubiliun, MD (Data curation: Supporting).
Christopher J. VandenBussche, MD, PhD (Data curation: Supporting).
Elizabeth D. Thompson, MD, PhD (Data curation: Supporting).
Michael S. Torbenson, MD (Data curation: Supporting).
Daniela S. Allende, MD (Data curation: Supporting).
Phoenix D. Bell, MD (Data curation: Supporting).
Cihan Kaya, PhD (Data curation: Supporting).
Abigail I. Wald, PhD (Conceptualization: Equal; Data curation: Equal; Formal analysis: Equal; Writing – original draft: Equal; Writing – review & editing: Equal).
Marina N. Nikiforova, MD (Conceptualization: Equal; Data curation: Equal; Formal analysis: Equal; Writing – original draft: Equal; Writing – review & editing: Equal).
Aatur Singhi, MD, PhD (Conceptualization: Lead; Data curation: Lead; Formal analysis: Lead; Writing – original draft: Lead; Writing – review & editing: Lead).

Conflicts of interest
These authors disclose the following: Aatur Singhi has received an honorarium from Foundation Medicine, Inc. Daniela S. Allende has received an honorarium and served as Advisory Board Member for Incyte. The remaining authors disclose no conflicts.

Funding
This study was supported in part by the Department of Defense (W81XWH-21-1-0709), National Cancer Institute, Early Detection Research Network (National Institutes of Health/National Cancer Institute 1U01CA200466), the Pittsburgh Liver Research Center at the University of Pittsburgh (National Institutes of Health/National Institute of Diabetes and Digestive and Kidney Diseases P30DK120531), the University of Pittsburgh Medical Center, the National Pancreas Foundation (Western Pennsylvania Chapter), and the Sky Foundation.

Supplementary Material and Methods

Study Samples

Study approval was obtained from the authors' respective institutional review boards. The anatomic pathology surgical archives from the departments of pathology at the University of Pittsburgh Medical Center (UPMC), Johns Hopkins Hospital, and University Medical Center Utrecht were queried for the diagnosis of ITPN. Cases with hematoxylin and eosin–stained slides and corresponding formalin-fixed paraffin-embedded tissue were retrieved and reviewed to confirm the diagnosis of an ITPN by a trained surgical pathologist with gastrointestinal tract and hepatopancreatobiliary subspecialty training (J.W.L., R.H.H., L.A.A.B., and/or A.D.S.). The diagnosis of an ITPN was based on the 2010 and 2019 World Health Organization classification of tumors of the digestive system.[1–3] Twenty-three ITPNs were identified as well as 4 matched preoperative pancreatic cyst fluid specimens that were submitted for molecular testing (PancreaSeqV2) through the Molecular and Genomic Pathology Laboratory at UPMC.[4]

Nucleic Acid Extraction

Nucleic acid extraction and subsequent DNA- and RNA-based targeted NGS were performed within the Clinical Laboratory Improvement Amendments–certified and College of American Pathologists–accredited Molecular and Genomic Pathology Laboratory at UPMC. Genomic DNA and RNA were isolated from formalin-fixed paraffin-embedded tissue (surgical resection specimens), and pancreatic cyst fluid was obtained by endoscopic ultrasound–guided fine-needle aspiration using the DNeasy Blood and Tissue kit on automated QIAcube instrument (Qiagen, Germantown, MD) or the MagNA Pure LC Total Nucleic Acid Isolation Kit (Roche, Indianapolis, IN) on Compact MagNA Pure (Roche). Extracted DNA and RNA were quantitated on the Glomax Discover using the QuantiFluor ONE dsDNA System and the QuantiFluor RNA system, respectively (Promega, Madison, WI).

DNA- and RNA-based Targeted NGS

Targeted NGS-based testing from isolated DNA and RNA was performed for all 23 cases within the Molecular and Genomic Pathology Laboratory at UPMC using the Oncomine Comprehensive Assay v3 (OCAv3) primers (Thermo Fisher Scientific, Waltham, MA) according to the manufacturer's protocol.[5] Amplicons were barcoded, ligated with specific adapters, and purified. DNA and RNA library quantity and quality checks were performed using the 4200 TapeStation (Agilent Technologies, Santa Clara, CA). The Ion Chef was used to prepare and enrich templates and enable testing using ion sphere particles on a semiconductor chip. Massive parallel sequencing was carried out on an Ion S5 XL System according to the manufacturer's instructions (Thermo Fisher Scientific), and data were analyzed with the Torrent Suite Software v5.12 for point mutations, small insertions/deletions, and copy number alterations.

Each variant was prioritized according to the 2017 Association for Molecular Pathology, American Society of Clinical Oncology, and College of American Pathologists joint consensus guidelines for interpretation of sequence variants in cancer using a tier-based system.[6] Tier I, II, and III variants were reported; however, only tier I and II variants were used for subsequent analysis.

The limit of detection of the assay was at 3% mutant allele frequency. The minimum depth of coverage for testing was 300 times. Copy number variation analysis was also performed as previously described.[7] The total depth of sequencing coverage of each sequenced region was normalized by the normal controls and calculated per sequenced case. A decrease in sequencing coverage below established cutoffs with a simultaneous presence of a sequence variant at high allele frequency was considered a copy number loss. In contrast, an increase in sequencing coverage above established cutoffs was interpreted as a copy number gain. A gene amplification was defined by the presence of $\geq$6 copies of a variant as previously described and validated using fluorescence in situ hybridization (FISH) analysis.[7,8]

Targeted RNA expression and fusions were evaluated using the Torrent Suite Software v5.12 and an in-house bioinformatics program, Variant Explorer (UPMC). The limit of detection of the RNA assay was 1%–5% tumor cells. More than 50 fusion-specific reads that cross the fusion breakpoint are required to make a positive fusion call.

Whole Transcriptome (RNA) Sequencing and Analysis

RNA sequencing libraries of cases 2, 4, 8, 10, 11, 13, 16, and 18–23 were prepared using the Illumina TruSeq RNA Exome Library Prep for Enrichment, according to the manufacturer's protocol. Cluster generation and paired-end sequencing were performed on an Illumina NextSeq 2000 using NextSeq 1000/2000 P2 Reagents (200 cycles) v3. For detection of gene fusions, sequencing data were analyzed using Chimerascan, FusionCatcher, and Star-Fusion algorithms integrated into an in-house developed bioinformatics pipeline for detection of clinically relevant fusions.[9–11] Analysis of sequencing data for gene expression was performed as previously described.[5,12]

For gene expression analysis, the filtered high-quality reads from HiSeq sequencing system were aligned to human genome (hg19-GRCh37) using TopHat aligner, and the number of reads mapped to each gene was calculated using RSeM and featureCounts tools.[13–15] From the read counts, the differential expression analysis was performed using the edgeR package.[16] The expression levels for target genes implicated in the epidermal growth factor receptor/extracellular signal-regulated kinase signaling pathways were evaluated as previously published.[5] Genes with a fold change of $>$2 and a $P < .05$ were selected as differentially expressed genes and used in pathway analysis.

MAML2 *FISH*

Break-apart FISH for cases 21–23 was used to evaluate for *MAML2* rearrangements as previously described.[17] Briefly, the *MAML2* break-apart probe consists of an 11q21 bacterial artificial chromosome, clones RP11-16K5 (Spectrum Orange) and RP11-676L3 (Spectrum Green), that map to the 5′ and 3′ ends of *MAML2*, respectively. Labeled clones were combined to create a dual-color, single-fusion probe set. Formalin-fixed paraffin-embedded sections were cut at 4 μm, mounted on positively charged slides, baked for 15 minutes at 90°C, and then deparaffinized in xylene. Slides were dehydrated in 100% ethanol and allowed to air dry. Pretreatment in 10 mM citric acid was followed by an NaCl protease treatment to remove proteins and non-DNA cellular components. The slide and probe were co-denatured and hybridized overnight. Slides were then washed, and 4′,6-diamidino-2-phenylindole counterstain was applied as well as a glass coverslip. Visualization of the FISH signals was accomplished by using a fluorescence microscope, and pictures were captured by using a FISH imaging system (CytoVision; Leica Biosystems, Buffalo Grove, IL). Two technologists experienced in FISH independently scored 50 tumor nuclei for each case with positivity defined as >15% of tumor cells demonstrating split signals (isolated green signals). Overlapping cells were excluded from analysis.

Supplementary References

1. Adsay NV, et al. Intraductal neoplasm of the pancreas. In: WHO classification of tumors of the digestive system. 4th ed. Lyon: IARC Press, 2010:304–313.
2. Basturk O, et al. Pancreatic intraductal tubulopapillary neoplasm. In: WHO classification of tumors of the digestive system. 5th ed. Lyon: IARC Press, 2019: 317–318.
3. Yamaguchi H, et al. Am J Surg Pathol 2009;33:1164–1172.
4. Singhi AD, et al. Gut 2018;67:2131–2141.
5. Singhi AD, et al. Gastroenterology 2020;158:573–582.
6. Li MM, et al. J Mol Diagn 2017;19:4–23.
7. Grasso C, et al. J Mol Diagn 2015;17:53–63.
8. Nikiforova MN, et al. NeuroOncol 2016;18:379–387.
9. Iyer MK, et al. Bioinformatics 2011;27:2903–2904.
10. Nicorici D, et al. bioRxiv 2014:011650.
11. Haas BJ, et al. bioRxiv 2017:120295.
12. Nikiforova MN, et al. Thyroid 2019;29:161–173.
13. Trapnell C, et al. Bioinformatics 2009;25:1105–1111.
14. Li B, et al. BMC Bioinformatics 2011;12:323.
15. Liao Y, et al. Bioinformatics 2014;30:923–930.
16. Robinson MD, et al. Bioinformatics 2010;26:139–140.
17. Seethala RR, et al. Am J Surg Pathol 2010; 34:1106–1121.

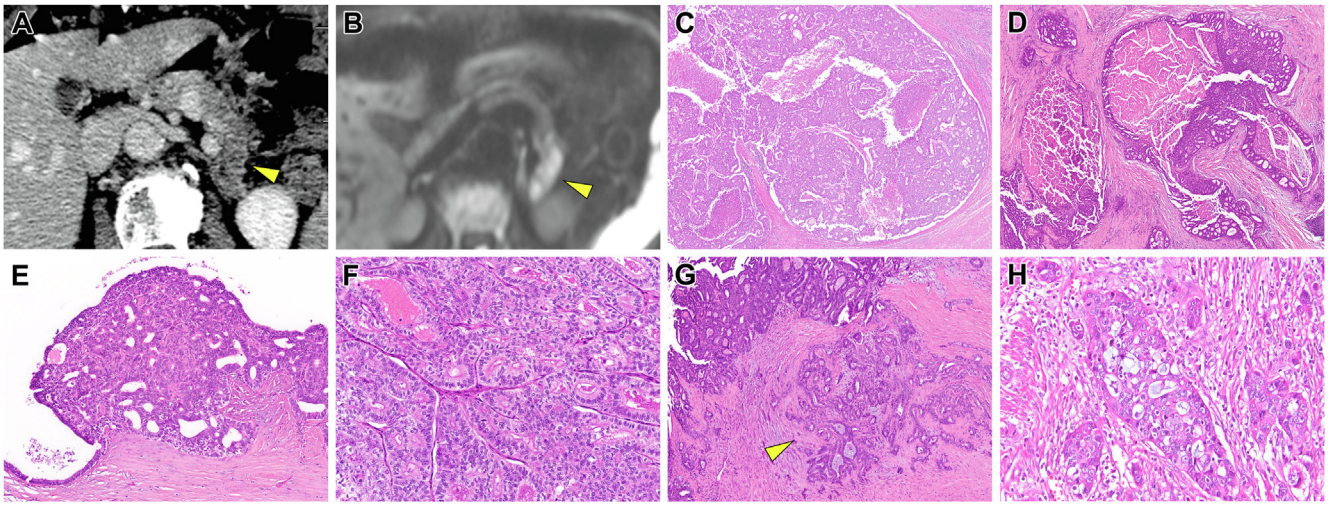

Supplementary Figure 1. Imaging and pathologic features of pancreatic ITPNs. Axial contrast-enhanced abdominal computed tomography of pancreatic ITPNs typically demonstrate a dilated main pancreatic duct that is involved by *(A)* a heterogeneous hypo-enhancing lesion (*yellow arrowhead*) of the distal pancreatic body and tail and *(B)* the lesion (*yellow arrowhead*) is associated with diffusion restriction. Histologically, ITPNs are characterized by an *(C)* intraductal nodular mass with scant mucin and *(D)* necrotic foci. At high magnification, these nodules are composed of a *(E)* tubulopapillary growth of ductal epithelium and *(F)* exhibit high-grade cytologic atypia. Further, ITPNs are often associated with *(G)* an invasive adenocarcinoma (*yellow arrowhead*) that *(H)* may also adopt a tubulopapillary/cribriform architecture.

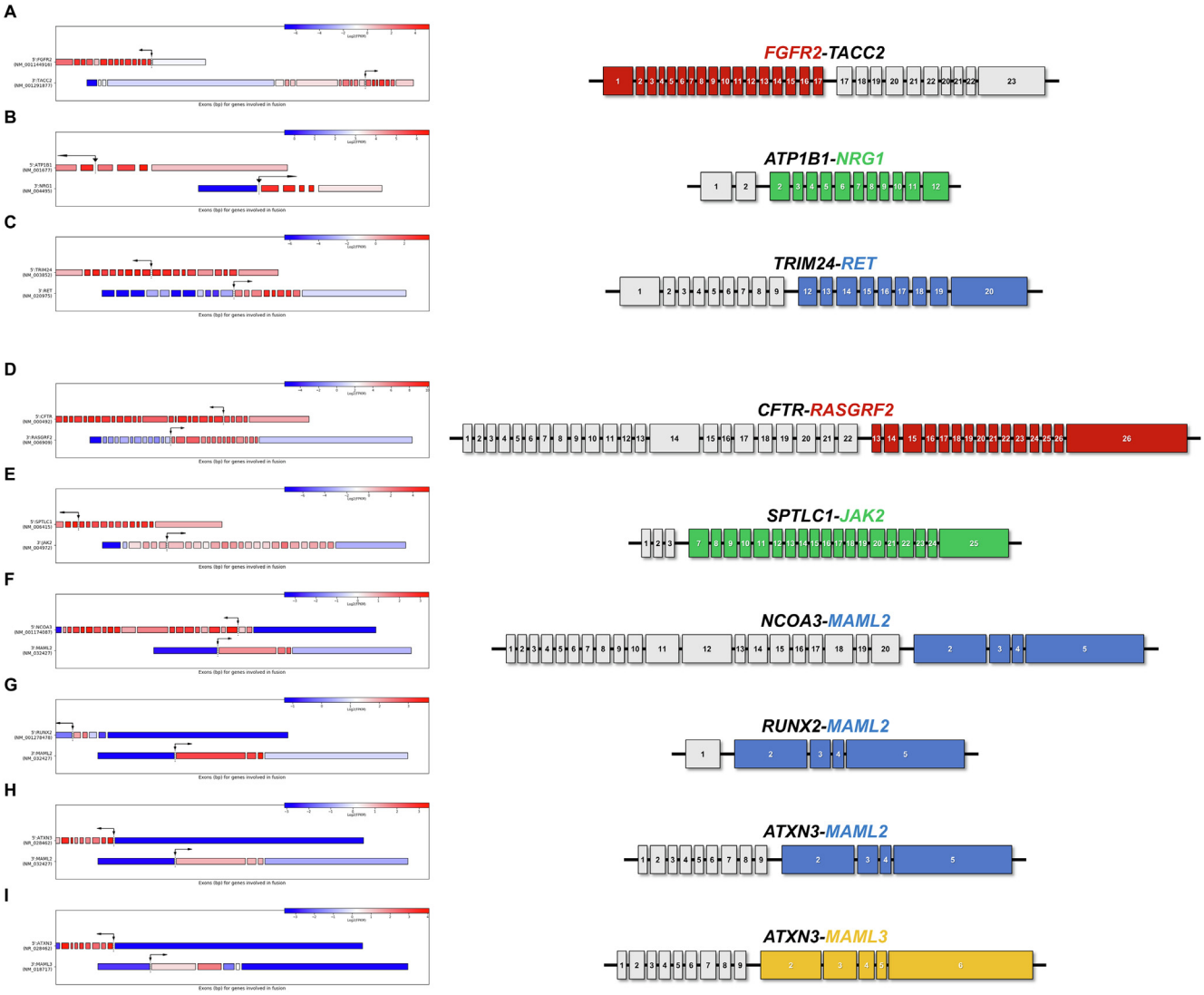

Supplementary Figure 2. Known MAPK fusion genes, such as those in *FGFR2 (A)*, *NRG1 (B)*, and *RET (C)* were identified by WTS of ITPNs. To the *left*, each *box* represents an exon of the designated gene with *black arrows* indicating the breakpoint. The color is indicative of relative expression levels, per exon basis, with *red* designating high expression and *blue* designating low expression. To the *right*, the specific exons of each gene are annotated. In addition to known fusion genes, WTS detected novel fusion genes that have been implicated within the MAPK signaling pathway to include *RASGRF2 (D)*, *JAK2 (E)*, *MAML2 (F–H)*, and *MAML3 (I)*.

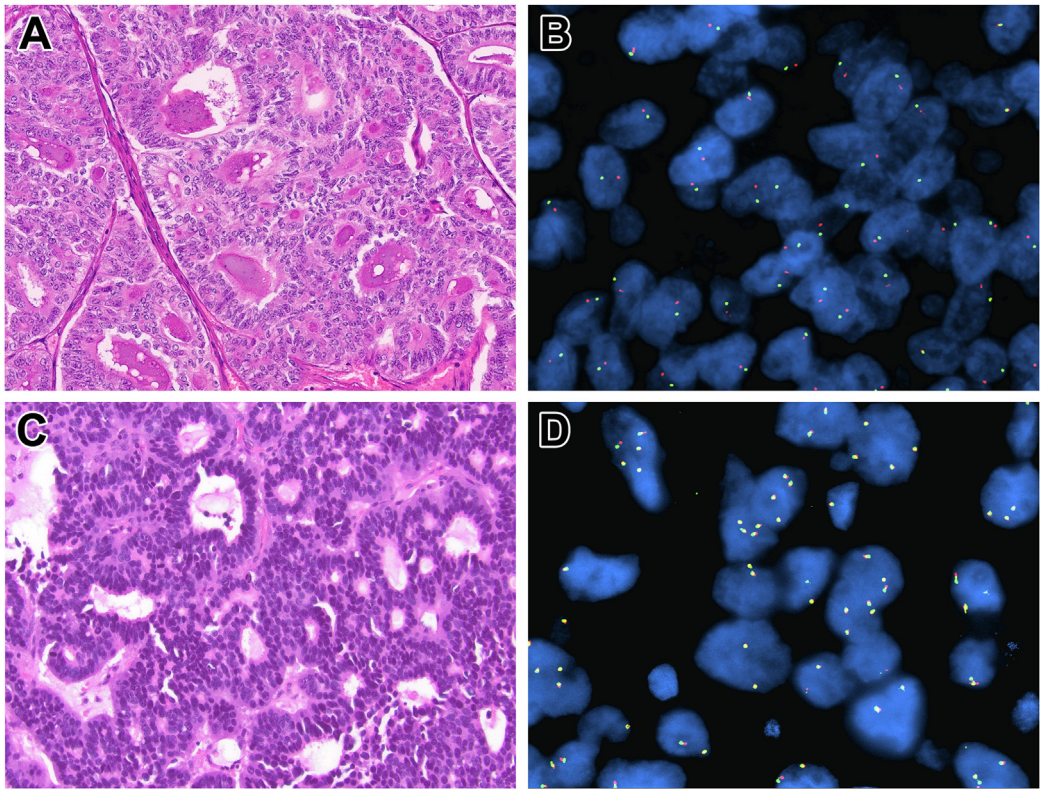

Supplementary Figure 3. *(A)* WTS of case 21 identified an *NCOA3-MAML2* fusion gene. *(B)* The *MAML2* rearrangement was confirmed using a break-apart FISH probe that exhibited isolated *orange* (5′ end of *MAML2*) and *green* (3′ end of *MAML2*) signals along with a concomitant chromosome 11q21 deletion. In comparison, *(C)* case 8 harbored an *ATP1B1-NRG1* fusion gene and demonstrated *(D)* wild-type *MAML2* (intact *yellow* signals due to overlapping *orange* and *green* signals).

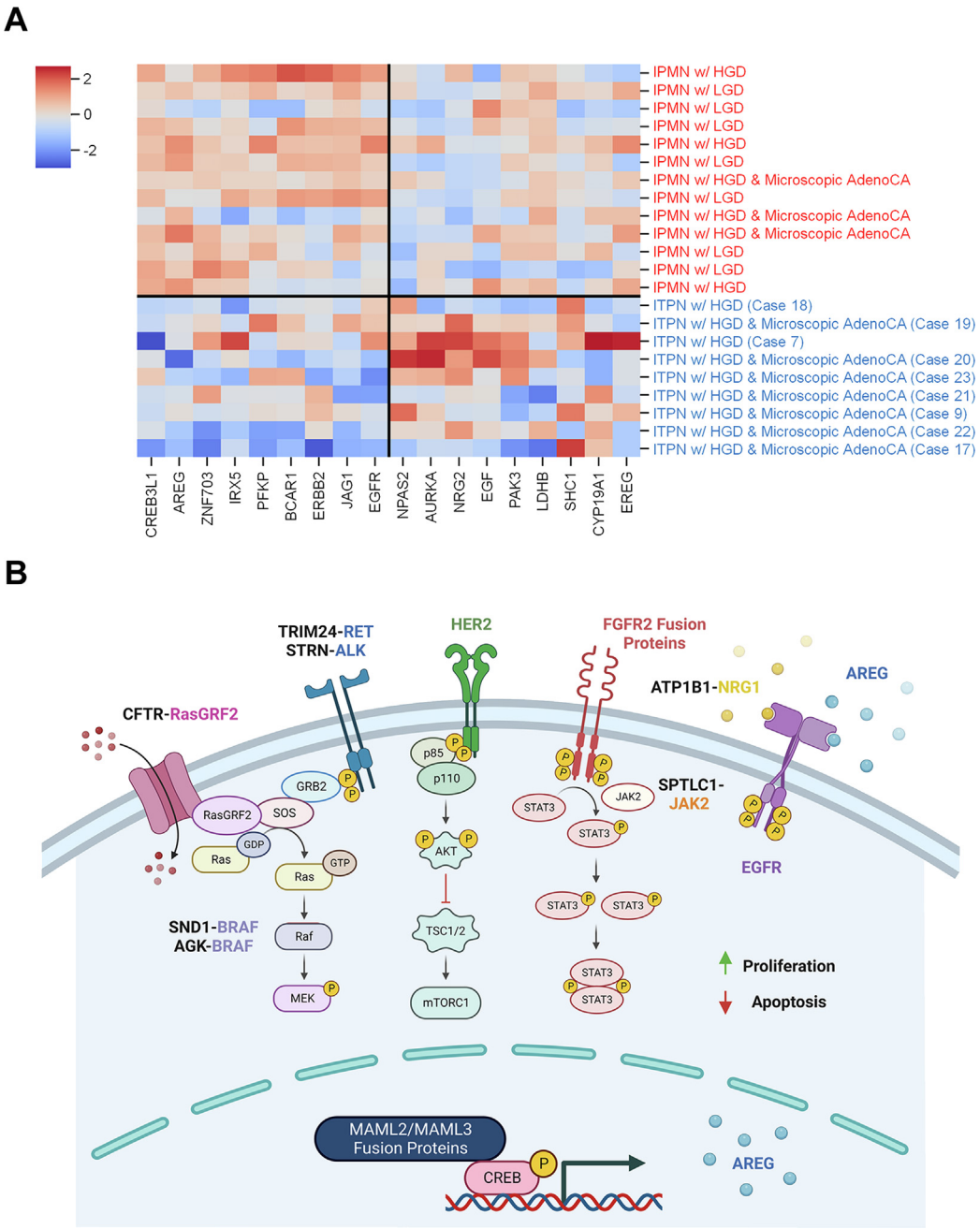

Supplementary Figure 4. Comparative WTS of intraductal papillary mucinous neoplasms (IPMNs; n = 13) and ITPNs (n = 9) and key genomic alterations associated with ITPNs to include affected signaling pathways. *(A)* Transcriptomic sequencing revealed increased expression of numerous genes implicated within multiple receptor tyrosine kinase (RTK) signaling pathways. However, ITPNs as compared with IPMNs exhibited differential expression for genes involved in epidermal growth factor receptor (EGFR)/extracellular signal-regulated kinase (ERK) signaling. *(B)* Despite the identification of multiple RTK signaling pathways and based on previous studies, the key genomic alterations that characterize ITPNs seem to converge onto the MAPK signaling pathway, which is known to regulate a variety of biologic processes, such as cell proliferation and survival. AdenoCA, adenocarcinoma; HGD, high-grade dysplasia; LGD, low-grade dysplasia.